

# RADIOMETRIC CALIBRATION OF THE MOMS-2P CAMERA

M. Schroeder, P. Reinartz, R. Müller

German Aerospace Center (DLR)  
Institute of Optoelectronics, Optical Remote Sensing Division  
D-82230 Wessling, Germany  
e-mail: Manfred.Schroeder@dlr.de  
Commission I, Working Group 1

## ABSTRACT

For the radiometric calibration of the MOMS-2P camera on board of the Russian MIR-station an inflight sun calibration method using a diffuser plate in front of the optics is applied. By tilting the diffuser plate by 20 degrees with respect to the entrance optics the direct sunlight is reflected into the optics. Prior to the absolute radiometric calibration of every pixel the image has to be corrected for relative radiometric disturbances along the scan lines. The reasons are the odd/even effect and the CCD typical non-uniformity. To correct for these effects relative calibration tables, derived from the diffuser plate calibration, are applied to the image. The applicability and stability of these tables is only given to an accuracy of about 1-2% in the nominal case. Therefore the remaining disturbances, probably caused by deficiencies of the internal electronic amplifier circuits and temperature variations, are removed using empirical methods. To correct for these random type of image failures, a digital filter in the spatial domain was developed. It is based on an averaging technique that acts in a large kernel size. Since there seems not to be complete linearity for very high and very low brightness levels, these levels have to be excluded from the averaging procedure. The image contrast and information content is less influenced than with other known filter techniques. In this paper the procedure to derive the level L1A Data is shown. After correcting for the relative radiometric differences the measured solar irradiance values can also be used for absolute calibration because the extraterrestrial spectrum of the sun is very well known. The methods to derive the absolute calibration factors are described and first results are presented.

## 1 INTRODUCTION

Data from optoelectronic instruments have to be radiometrically equalized before they can be used for evaluation purposes. In the case of the MOMS-2P sensor there are 8 different CCD-arrays with 6000 CCD-elements each. To get a sensitivity profile of such an array there are several possibilities:

- in laboratory:  
using an integrating sphere, a flat fielding process or a solar light simulator and a diffuser plate, where the whole field of view is illuminated.
- in orbit:  
using a diffuser plate for the incoming sun radiation or internal lamps.

In the case of MOMS-2P several measurements have been made with two different methods in laboratory. The calibration values derived from these measurements could not be used for the data correction successfully. This may be due to changes in the electronic data chain between the calibration measurements and the in-orbit data acquisition (the time interval between these two events has been one year and more). Therefore the best possibility was to use sun calibration data during in-orbit measurements.

The typical effects which disturb the data recording of the CCD-array devices and the optics are:

- the odd-even effect, this means that there are two different amplifier circuits for the signal coming from either the odd CCD-elements or the even CCD-elements

- the non-uniformity of the CCD-elements, this means that the single CCD-detectors have a different sensitivity
- the light fall off of the optics at the borders of the CCD-array
- electronic instabilities due to temperature variations and read-out via the correlated double sampling technique

The first part of this paper deals with the procedures for correcting these effects. The goal is to determine tables for relative calibration of every channel which are valid for all intensity values. These tables are necessary for the production of L1A and L1B data.

In the second part it will be shown how absolute calibration factors can be obtained from measuring the sun irradiance to convert the relatively corrected data into radiance values. One prerequisite for deriving the absolute calibration factors is that the relation between input- and output signal is linear. Whether this linear relation really exists will be investigated in the last part of this paper.

## 2 RELATIVE RADIOMETRIC CALIBRATION

The data which are gathered during the in-flight sun calibration measurements have the same format like the real images taken from the earth surface. For the purpose of these investigations, calibration data from two subsequent days have been used (28th and 29th January 1997). Both data sets were acquired during the MIR-station was crossing the day-night borderline at a sunset. These data were also used for absolute calibration. This means that during a time period of about 20 seconds, the full intensity of the incoming sun

radiation is reduced to zero. 20 seconds is equivalent to 8000 scan lines.

The first procedure is to subtract the dark current, which is measured before each data take and is different for each pixel.

After this, the relative calibration factor can be evaluated by the following formula:

$$r_i^{-1} = \frac{\overline{DN}_i}{\frac{1}{N} \sum_{k=1}^N \overline{DN}_k} \quad (1)$$

$\overline{DN}_i$  mean value of column  
 $N$  Number of columns  
 $r_i$  relative calibration factor for column  $i$

The relative calibration- or equalization factor  $r_i$  can then be used in the following way to correct a scene.

$$g_i^{calibrated} = r_i \cdot g_i^{raw} \quad (2)$$

$g_i$  pixel value of column  $i$

The formula (2) can be used under the assumption that the above mentioned signal disturbing effects are of multiplicative nature. This is only true, if the sensor reacts linear or for the sensitivity niveau in which it acts linear. Figure 1 shows the result for the calibration values of channel 1 for only the even-part of the CCD-array. The light fall off at the borders can be seen clearly, as well as the non-uniformity of the chip.

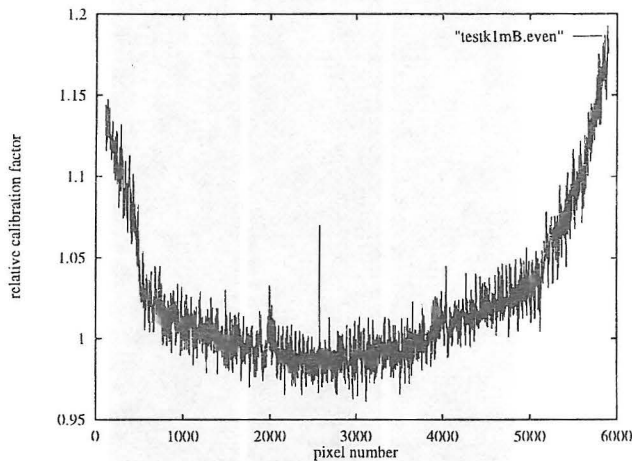


Figure 1: Relative calibration factors of channel 1 (only even pixels)

## 2.1 INTENSITY DEPENDANCE OF THE CALIBRATION TABLES

As mentioned above, the data set contains sun data with different intensities due to the sunset during the data take. To verify the stability of the sensor, several calibration tables have been calculated for different levels of intensities. The mean intensities for this investigation have been from 100% (full sun) to 20% illumination in five steps. Figure 2 shows the resulting calibration values for five intensities. Only 10 CCD-elements are shown for a better demonstration of the effects. It can be seen clearly that there is a difference for

every single calibration factor and that the tendency for the changes is not uniform for every CCD- element. This shows a kind of statistical behaviour of the read-out electronics which is in the order of about 1-2%.

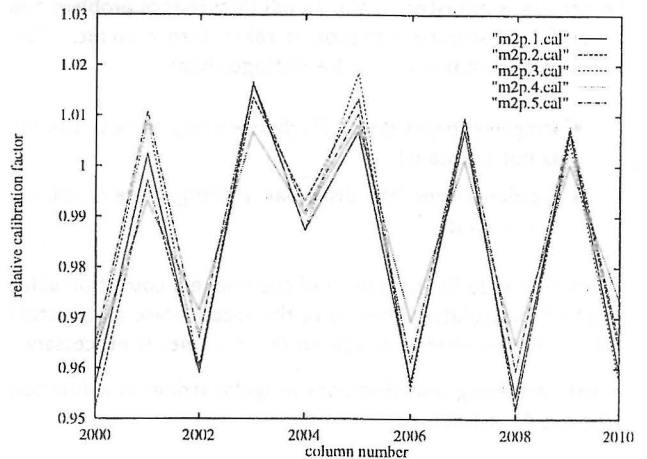


Figure 2: Relative calibration factors of channel 1 (only even pixels) derived at different intensities with gain level 4 (max. gray value 140)

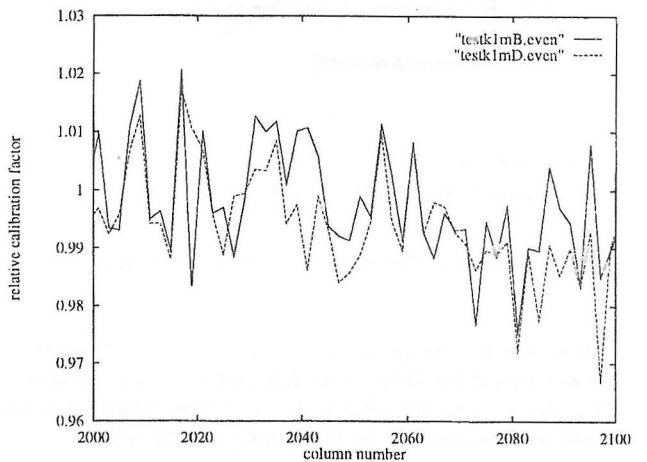


Figure 3: Relative calibration factors of channel 1 (only even pixels) on different days

A similar behaviour can be seen in the data sets of two different days. Figure 3 shows the results of the calibration value calculation for the same array at two consecutive days. For some CCD-elements the same values can be observed, while for others the difference is also up to about 2%. This means that the accuracy of the relative calibration procedure is also in the order of 1-2%. The result is that after applying the relative calibration factors there is still some along track striping in the images which has to be corrected for an optimal use of the images for any kind of evaluation.

## 2.2 EMPIRICAL METHOD FOR OPTIMIZED IMAGE CORRECTION

A digital filter in the spatial domain can be designed to correct for this kind of image disturbance [1]. Based on an averaging method inside a large kernel size it acts as a local filter whose kernel size is adjusted to the actual disturbance problem and its preferred striping direction is taken into account. Two types of disturbances must be distinguished:

- irregular stripes (the disturbance along a line or column is not constant)
- regular stripes (the disturbance along a line or column is constant)

In the first case for each pixel of the image a correction value has to be calculated whereas in the second case a correction value for each pixel in a column (or in a line) is necessary.

For the following considerations irregular stripes in y-direction (see Fig.4) is assumed.

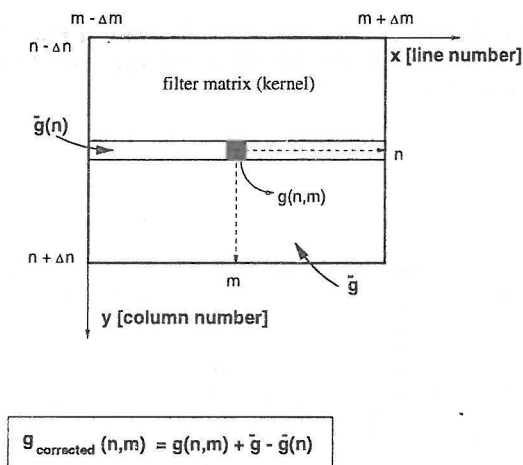


Figure 4: Principle of the filter technique

In this case for each pixel  $g(n, m)$  (located at the center of the window) in the image a window (kernel) of size  $(2 \cdot \Delta m + 1)(2 \cdot \Delta n + 1)$  for the filter matrix is defined (Note: the size of the window depends on the stripe characteristics).

For each pixel  $g(n, m)$  an additive correction value  $d(n, m)$ , derived from the surrounding window, is calculated using the formula

$$d(n, m) = \bar{g} - \bar{g}(n) \quad (3)$$

where

$$\bar{g}(n) = \frac{1}{\Delta m + 1} \sum_{i=m-\Delta m}^{m+\Delta m} g(n, i)$$

mean value of column  $n$

$$\bar{g} = \frac{1}{\Delta n + 1} \sum_{j=n-\Delta n}^{n+\Delta n} \bar{g}(j) \quad (4)$$

mean value of kernel

Because of this stripe direction the mean value of a column must be used. The correction of the pixel  $g(n, m)$  is carried out by

$$g_{corrected}(n, m) = g(n, m) + d(n, m) \quad (5)$$

This removes the image stripes without affecting the image content and the image contrast is nearly unchanged. The value of  $d(n, m)$  can be interpreted as the adjustment of the mean value of column  $n$  to the mean window value.

In the case of MOMS-2P the window size in line direction is best chosen in the order of 10 to 14 columns while in column direction the whole image lines are taken. Only for the highest and lowest intensities the sensor seems not to act linear. For saturated areas like clouds this is nominal. It has to be taken care of when calculating the mean values that this part is excluded. Due to the non-linearity effects also the low brightness values (up to about 20 grey values) have to be excluded from the filtering procedure. After this kind of correction nearly all striping is gone, only in the saturated and the low level part a rest striping can be seen. In Figure 5 a comparison of the data before and after correction is shown. This is demonstrated with sun calibration data which were calibrated with a calibration table from another date.

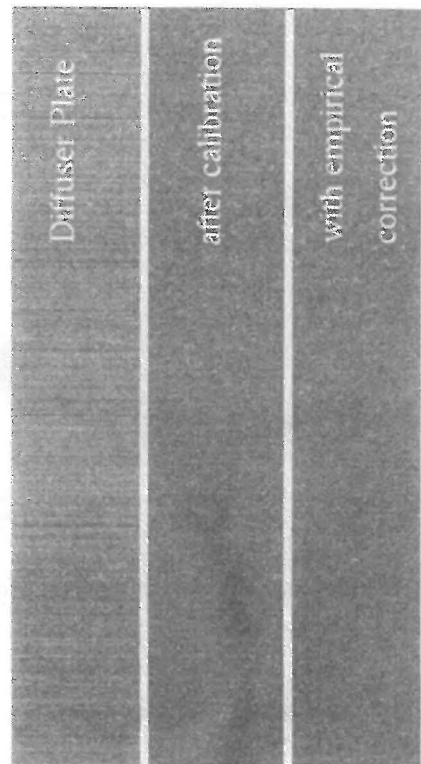


Figure 5: Image equalization of sun calibration data before and after empirical correction

## 3 ABSOLUTE RADIOMETRIC CALIBRATION

The task of absolute radiometric calibration can be defined in general form as follows:

Absolute radiometric calibration is performed by rationing the digital number (DN) output of a sensor with the value of an accurately known, uniform radiance field at its entrance pupil. The full field of view should be filled with the radiance source. [2]

Probably this last condition was not fulfilled during the MOMS laboratory calibration.

The corresponding formula to the above definition is:

$$DN = A \cdot L \quad (6)$$

- $L$  is the radiance entering the optics of the sensor which must precisely be known
- $DN$  is the corresponding sensor signal in digital numbers
- $A$  is the absolute calibration factor which has to be determined and which is given in digital numbers per radiance units

The concept is based on the theoretical model that the relation between  $DN$  and  $L$  is linear. This is valid for most CCD sensors, but this linear relation should be checked in the calibration process (chapter 4).

It should be mentioned that the  $DN$  value in (6) is the value after

- subtraction of the dark current
- applying the relative calibration which takes into account varying sensitivity of the detector elements of the CCD line (chapter 2)
- correcting for other gray value non uniformities (chapter 2.2)

The knowledge of absolute calibration and also the temporal change of the calibration coefficient is especially important if one tries to detect changes on the ground with time sequential images. If the calibration is not known, then changes in the sensors response are likely to be incorrectly attributed to changes in the observed scene [2].

### 3.1 SUN CALIBRATION

For sun calibration the protection cover of the MOMS - optics could be used [Fig.6]. The inner side of this cover is coated with grey spectralon material which is a diffuse reflector.

For calibration the lid was tilted by 20 degrees. During calibration the MIR- station flew in a so called inertial attitude in which the angle between the normal vector of the cover plate and the sun remained constant.

In this attitude the optical axis was not looking vertical down to the earth.

This inner coating of the cover plate with spectralon was originally forseen for controlling the stability of the laboratory calibration.

### 3.2 SUN DIRECTION

To determine the sun irradiance on the diffuser plate the angle between the normal vector of the plate  $r_F$  and the direction

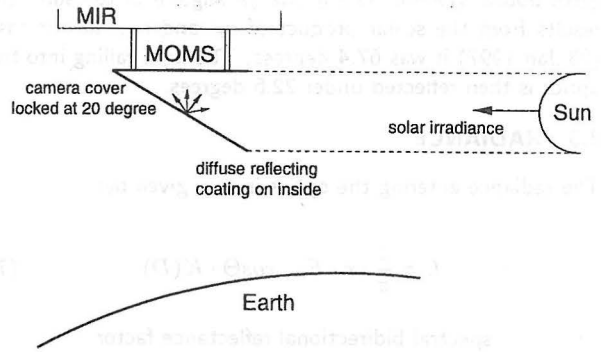
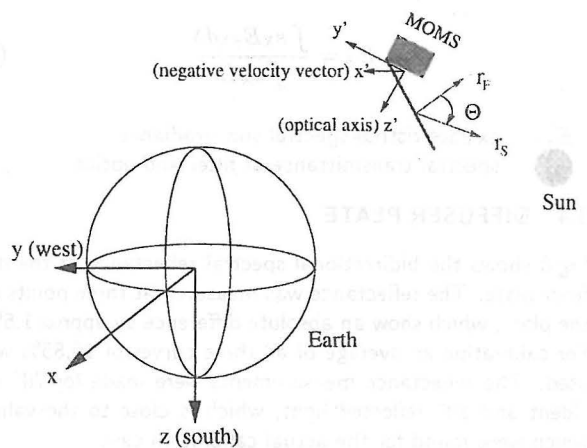


Figure 6: MOMS-2P with tilted cover for sun calibration

of the sun  $r_S$  had to be known [Fig.7]. For this purpose the attitude of a sensor coordinate system with respect to an earth bound geocentric system was given by the Russian ground control center. In addition the universal time (UTC) for the data take was available.



Attitude data of  $(x', y', z')$  with respect to  $(x, y, z)$  are given:

1. Rotation around y-axis, clockwise: 64.624
2. Rotation around x-axis, counterclockwise: 5.953
3. Rotation around z-axis, counterclockwise: 335.234

$$r_F = (0.899, -0.243, -0.365)$$

UTC - time: 27 Jan 97,7:30

$$r_S = (0.314, -0.894, 0.319)$$

Figure 7: Coordinate Systems to determine the incidence angle of the sun

The two systems were rotated with respect to each other by three rotations around their axis in a certain order which is indicated in Fig.7. The rotation angles were given [see Fig.7] and could be used for calculating the normal-vector of the diffuser plate.

From the given UTC-time the sun direction could be calculated for a plane tangential to the equator and to the Greenwich meridian. This gives also the sun direction  $r_S$  in the

earth bound system. The incidence angle  $\theta$  of the sun light results from the scalar product of  $r_F$  and  $r_S$ . In our case (28 Jan 1997) it was 67.4 degrees. The light falling into the optics is then reflected under 22.6 degrees.

### 3.3 RADIANCE

The radiance entering the optics is now given by:

$$L = \frac{1}{\pi} \cdot r \cdot E_S \cdot \cos\Theta \cdot K(D) \quad (7)$$

- $r$  spectral bidirectional reflectance factor in a certain spectral band
- $E_S$  sun irradiance in a certain spectral band
- $\cos\Theta$  takes into account the projection of the sun light on the tilted plate
- $K(D)$  takes into account the change of the earth-sun distance during the year and depends on the day of the year.  
The yearly variation in distance is  $\pm 3\%$ .

$E_S$  is derived by integrating the spectral irradiance of the sun over the spectral bandwidth.

$$E_S = \frac{\int s_\lambda E_{S\lambda} d\lambda}{\int s_\lambda d\lambda} \quad (8)$$

- $E_{S\lambda}$  extraterrestrial spectral sun irradiance
- $s_\lambda$  spectral transmittance of filter and optics

### 3.4 DIFFUSER PLATE

Fig.8 shows the bidirectional spectral reflectance of the diffuser plate. The reflectance was measured at three points on the plate, which show an absolute difference by approx 1.5%. For calibration an average of all three curves of 16.85% was used. The reflectance measurements were made for  $70^\circ$  incident and  $20^\circ$  reflected light, which is close to the values which were found for the actual calibration case.

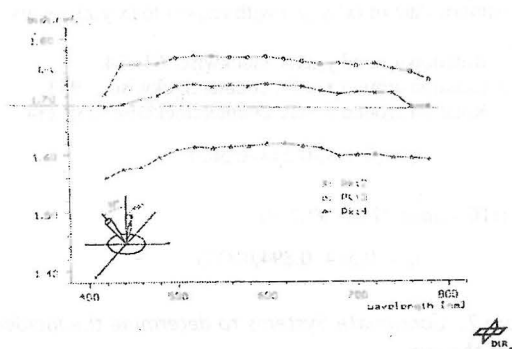


Figure 8: Bidirectional reflectance of diffuser plate

### 3.5 SUN IRRADIANCE

The exo - atmospheric spectral irradiance  $E_{S\lambda}$  is very well known and provided by Neckel/Labs [3] in tables in 2nm steps. This values are widely used for sun calibration and radiation transfer models of the atmosphere (s. upper curve of Fig.9).

Channel [#]	$\Delta\lambda$ [nm]	$A[\frac{DN}{mW \cdot m^{-2} \cdot sr^{-1} \cdot nm^{-1}}]$
1	440 - 505	3.521
2	530 - 575	3.704
3	645 - 680	2.500
4	770 - 810	6.098

Table 1: Absolute Calibration Factor A for Gain 4

In addition the relative spectral transmittance curves for the filters of the four spectral bands of MOMS-2P are drawn in Fig.9. Multiplying the spectral irradiance with the filter curves and integrating over the spectral bandwidth of the filters lead to the irradiance in each channel. The numerical values in  $\frac{mW}{m^2 \cdot nm}$  are indicated over each filter curve in Fig.9.

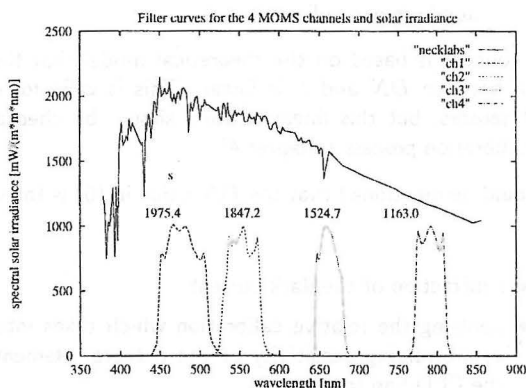


Figure 9: Filter Curves and Solar Irradiance

### 3.6 CALIBRATION FACTORS

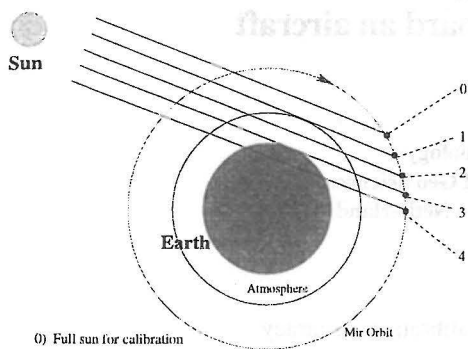
With the known reflectance and irradiance in each channel the radiance entering the optics can be computed (equ. 7). Dividing the recorded Digital Number of the sensor output by this radiance gives the absolute calibration coefficient  $A$  in table 1. The values in table 1 were derived for a gain factor of 4.

This are the very first calibration results and further measurements have to be made to check the reliability of these values.

## 4 IN-/OUTPUT LINEARITY

To check whether a linear relation between the sensor's digital output and the radiance input exists it was tried to use the event of a sunset. Fig.10 shows in principle what happens to the sun light during the sunset event if seen from a sensor in a space orbit.

- In position 1:  
The full sun disk is still be seen but the light is attenuated by the upper atmosphere
- In position 2:  
The sunlight is diminished by two effects:



- 0) Full sun for calibration
- 1) Sun light affected by atmosphere
- 2) Begin of sunset and atmospheric effects
- 3) Atmospheric transmittance constant
- 4) Twilight effects

Figure 10: Sun irradiance at orbiting sensor during sunset

- the area of the sun disk decreases because it is partly covered by the earth and
- by increasing atmospheric attenuation

- In position 3:  
The atmospheric transmittance is nearly constant and the sun irradiance decreases proportional with the decreasing area of the sun disk. This positions in orbit can be used to check the linearity.
- In position 4:  
No direct sun is seen. Only some scattered light from twilight effects.

The relative area of the sun disk as seen by the sensor can easily be calculated because the positions of the sensor and the sun are known as well as the radii of the earth and the sun.

The sun calibration was carried out before the MIR - station flew through the sunset into the dark night side of the earth. The decreasing light during this sunset was also recorded by the MOMS - sensor.

The results of these measurements are shown in Fig.11 and Fig.12 for channel 1 respectively channel 4. The upper curve shows the relative area of the sun disk as seen from the sensor. The relative area is indicated on the left y-axis.

On the x-axis the time is given in sec. The sunset event lasts about 15 sec. The lower curve is the sensor output in digital numbers.

The sections 1 to 4 of Fig.11 and Fig.12 correspond to the orbit positions as shown in Fig.10.

In section 3 the atmospheric transmittance is nearly constant and the irradiance is nearly direct proportional to the sun disk area.

In this section the sensor output decreases in the same manner as the solar irradiance. This is a strong indication that the sensor reacts linear. The slight deviations seem to be remaining atmospheric effects.

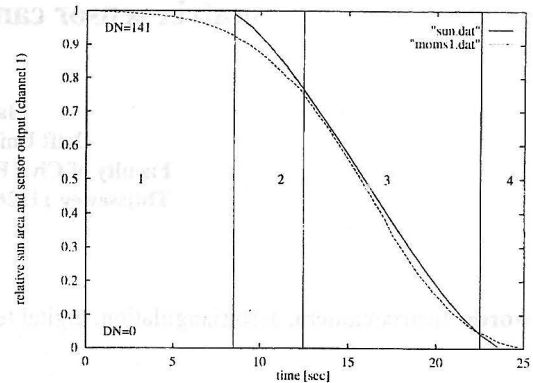


Figure 11: Sun surface area (~ irradiance) and sensor output (DN: 141-0)

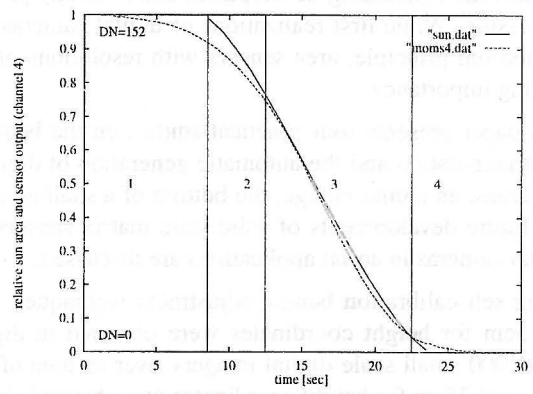


Figure 12: Sun surface area (~ irradiance) and sensor output (DN: 152-0)

## REFERENCES

- [1] P. Reinartz, R. Müller, M. Schroeder, V. Amann: "Correction of random signal disturbances in line scanner imagery" Seventh International Symposium, Physical Measurements and Signatures in Remote Sensing, 7-11 April 1997, Courchevel, France
- [2] Dinguirard, M.: "Optical Sensor Calibration", Seventh International Symposium, Physical Measurements and Signatures in Remote Sensing, 7-11 April 1997, Courchevel, France
- [3] Neckel, H.; Labs, D.: "The Solar Radiation between 3300 and 12500 Å", Solar Physics 90 (1984) 205-258